SPECTRAL ESTIMATION FOR MAGNETIC RESONANCE SPECTROSCOPIC IMAGING WITH SPATIAL SPARSITY CONSTRAINTS

Qiang Ning[1], *Chao Ma*[2], *and Zhi-Pei Liang*[1,2]

[1]Department of Electrical and Computer Engineering, and
[2]Beckman Institute for Advanced Science and Technology, University of Illinois at Urbana-Champaign

ABSTRACT

This paper addresses the long-standing spectral quantitation problem in magnetic resonance spectroscopic imaging (MRSI). Although a large body of work has been done to develop robust solutions to the problem for practical MRSI applications, the problem remains challenging due to low signal-to-noise ratio (SNR) and model nonlinearity. Building on the existing work on the use of prior knowledge (in the form of spectral basis) for spectral estimation, this paper reformulates spectral quantitation as a joint estimation problem, and utilizes a regularization framework to enforce spatial constraints (e.g., spatial smoothness or transform sparsity) on the spectral parameters. Simulation and experimental results show that the proposed method, by exploiting both the spatial and spectral characteristics of the underlying signals, can significantly improve the estimation accuracy of the spectral parameters over state-of-the-art methods.

Index Terms— MRSI, spectral estimation, spatial regularization, sparsity constraint, Cramér-Rao bound

1. INTRODUCTION

MRSI is a unique tool for non-invasive acquisition of biochemical information (e.g., concentration of metabolites) from biological systems, and spectral quantitation is one of the key underlying problems. This problem is challenging due to low SNR and model nonlinearity. Significant efforts have been made to address this problem in order to obtain robust estimates of spectral parameters, i.e., metabolite concentrations, T_2 relaxation time constants, and resonance frequencies. Earlier linear prediction-based methods (e.g., HSVD [1], HLSVD [2], LPSVD [3], and HTLS [4]) solve the underlying nonlinear optimization problem effectively but perform poorly on MRSI data of low SNRs. State-of-the-art methods (e.g., VARPRO [5], LCModel [6], QUEST [7], AQSES [8], Soher et al. [9], etc.) enforce stronger spectral constraints (in the form of spectral basis) and provide much better estimates of the spectral parameters over the linear prediction-based methods. While VARPRO, LCModel, and QUEST have been successfully used for processing practical MRSI data, they have large estimation variances in the regime of very low SNRs, significantly limiting their practical utility in high-resolution MRSI applications.

This paper addresses this problem by reformulating spectral quantitation as a joint estimation problem (in contrast to the existing methods that estimate the spectral parameters voxel by voxel independently). The new formulation enables the use of known spatial characteristics of metabolite distributions (e.g., smoothness or transform sparsity) for improved spectral estimations. More specifically, we use a regularization framework to enforce spatial constraints on spectral estimation and solve the resulting regularized least-squares problem efficiently in a two-step procedure. We have carried out a performance analysis of the proposed method using constrained Cramér-Rao bound (CRB) [10, 11], which shows the theoretical benefits of using spatial constraints for improving spectral estimation. The improved performance of the proposed method over one of the state-of-the-art methods, VARPRO [5], has been validated using both simulation and experimental data.

The rest of this paper is organized as follows. Section 2 describes the signal model, problem formulation, and proposed solution. Section 3 discusses the performance of the proposed method based on our simulation and experimental studies and theoretical analysis, which is followed by the conclusion of this paper in section 4.

2. PROPOSED METHOD

2.1. Problem Formulation

The measured time-domain MRSI data $d(\boldsymbol{x}, t)$ at spatial location $\boldsymbol{x}_p$ and time instant t_q for $p = 1, \cdots, P$, and $q = 1, \cdots, Q$, from a sample with N metabolites can be expressed as

$$d(\boldsymbol{x}_p, t_q) = \sum_{n=1}^{N} a_n(\boldsymbol{x}_p) e^{-t_q/T^*_{2,n}(\boldsymbol{x}_p)} e^{-i2\pi\Delta f(\boldsymbol{x}_p)t_q} \varphi_n(t_q) + \xi_{pq}, \tag{1}$$

where ξ_{pq} represents measurement noise (often assumed to be Gaussian), $a_n, T^*_{2,n}$, and φ_n represent the concentration (weighted by echo-time), T^*_2 relaxation time, and basis function for the nth metabolite, respectively, and $\Delta f(\boldsymbol{x}_p)$ is the frequency shift caused by B_0 field inhomogeneity. Here, φ_n is assumed to be known because it can be obtained from either quantum simulation (e.g., GAVA [12]) or in vitro experiments. Note that we have intentionally left out the baseline components in this signal model for simplicity.

For notation convenience, Eq. (1) can be written in a vector-matrix form as

$$\boldsymbol{d}_p = \mathbf{K}(\boldsymbol{\theta}_p)\boldsymbol{a}_p + \boldsymbol{\xi}_p, \quad p = 1, \cdots, P, \tag{2}$$

where $\boldsymbol{d}_p$ contains all the measured data at location $\boldsymbol{x}_p$ put in a vector form, and similarly, $\boldsymbol{a}_p$ and $\boldsymbol{\xi}_p$ are the concentration vector and noise vector, respectively. $\mathbf{K}(\boldsymbol{\theta}_p)$ is the model matrix with $\boldsymbol{\theta}_p$ containing all the nonlinear unknown parameters (i.e., $T^*_{2,n}$) at location $\boldsymbol{x}_p$ as defined in (1).

The goal of spectral quantitation in MRSI is to determine $\boldsymbol{a}_p$ and $\boldsymbol{\theta}_p$ from $\boldsymbol{d}_p$. This is done in existing methods by solving the following optimization problems (or maximum likelihood estimation problems for Gaussian noise):

$$(\hat{\boldsymbol{a}}_p, \hat{\boldsymbol{\theta}}_p) = \arg\min_{\boldsymbol{a}_p, \boldsymbol{\theta}_p} \|\boldsymbol{d}_p - \mathbf{K}(\boldsymbol{\theta}_p)\boldsymbol{a}_p\|_2^2, \tag{3}$$

for $p = 1, 2, \cdots, P$. In the absence of any spatial constraints, the above estimation problems can be solved independently. Here, we propose to solve these estimation problems jointly so that we can impose spatial constraints on both $\boldsymbol{a}_p$ and $\boldsymbol{\theta}_p$. Let $\boldsymbol{d} = \left[\boldsymbol{d}_1^T,\ \boldsymbol{d}_2^T,\ \cdots,\ \boldsymbol{d}_P^T\right]^T$, $\boldsymbol{a} = \left[\boldsymbol{a}_1^T,\ \boldsymbol{a}_2^T,\ \cdots,\ \boldsymbol{a}_P^T\right]^T$, and $\mathbf{K}(\boldsymbol{\theta}) = [\mathbf{K}(\boldsymbol{\theta}_1) \mid \mathbf{K}(\boldsymbol{\theta}_2) \mid \cdots \mid \mathbf{K}(\boldsymbol{\theta}_P)]$, we reformulate the spectral quantification problem as

$$(\hat{\boldsymbol{a}}, \hat{\boldsymbol{\theta}}) = \arg\min_{\boldsymbol{a},\boldsymbol{\theta}} \|\boldsymbol{d} - \mathbf{K}(\boldsymbol{\theta})\boldsymbol{a}\|_2^2 + \mathrm{R}(\boldsymbol{a}, \boldsymbol{\theta}), \tag{4}$$

where $\mathrm{R}(\boldsymbol{a}, \boldsymbol{\theta})$ is a regularization functional to absorb spatial constraints on $\boldsymbol{a}$ and $\boldsymbol{\theta}$. In the present study, we focus on imposing smoothness constraints. This is motivated by the fact that in most MRSI data obtained from biological samples, spatial distributions of T_2^* relaxation time and of metabolite concentration within a tissue are rather smooth. More specifically, we propose to impose spatial constraints on $\boldsymbol{\theta}$ and $\boldsymbol{a}$ by sequentially solving the following two regularized least-squares problems:

$$\hat{\boldsymbol{\theta}} = \arg\min_{\boldsymbol{\theta}} \frac{1}{2}\|\boldsymbol{d} - \mathbf{K}(\boldsymbol{\theta})\mathbf{K}(\boldsymbol{\theta})^{\dagger}\boldsymbol{d}\|_2^2 + \lambda\|\mathbf{W}_{\boldsymbol{\theta}}\boldsymbol{\theta}\|_2^2, \tag{5}$$

$$\hat{\boldsymbol{a}} = \arg\min_{\boldsymbol{a}} \frac{1}{2}\|\boldsymbol{d} - \mathbf{K}(\hat{\boldsymbol{\theta}})\boldsymbol{a}\|_2^2 + \eta\|\mathcal{W}_{\boldsymbol{a}}\{\boldsymbol{a}\}\|_1, \tag{6}$$

where "†" represents the Moore-Penrose pseudo inverse, λ and η are regularization parameters, the weighting matrix $\mathbf{W}_{\boldsymbol{\theta}}$ (derived from one or multiple reference images) is used to preserve edges (see [13] for details), and $\mathcal{W}_{\boldsymbol{a}}$ is a sparsifying operator, e.g., the wavelet transform, total variation (TV) transform, or total generalized variation (TGV) transform [14]. The formulation in (5) and (6) decouples the estimation of the nonlinear parameter ($\boldsymbol{\theta}$) from that of the linear parameter ($\boldsymbol{a}$) using the variable projection strategy, significantly improving the computational efficiency.

2.2. Solution Algorithm

The joint quantitation problem in (5) and (6) is much larger than the individual quantitation problems in (3), so it is desirable to solve them efficiently. The problem in (5) is a weighted ℓ_2-norm regularized nonlinear least squares problem, which can be solved using a quasi-Newton method where only gradient evaluation is required. We used the limited memory Broyden-Fletcher-Goldfarb-Shanno (L-BFGS) algorithm [15] to solve (5) because of its computational efficiency and relatively low memory usage.

After $\boldsymbol{\theta}$ is estimated, we then solve the ℓ_1-norm regularized least-squares problem in (6) using an alternating direction method for multiplier (ADMM) [16]. For simplicity, we present the algorithm for the case that $\mathcal{W}\{\boldsymbol{a}\}$ in (6) is a linear operator of $\boldsymbol{a}$ (e.g., the wavelet and TV transform) and can thus be represented in a matrix form, i.e., $\mathcal{W}_{\boldsymbol{a}}\{\boldsymbol{a}\} = \mathbf{W}_{\boldsymbol{a}}\boldsymbol{a}$. The proposed algorithm can be easily extended to the case that $\mathcal{W}\{\boldsymbol{a}\}$ represents the TGV transform as in [14, 16]. As proposed by Guo et al. [16], we introduce an auxiliary variable $\boldsymbol{u}$, so that (6) is equivalent to

$$\min_{\boldsymbol{a},\boldsymbol{u}} \frac{1}{2}\|\boldsymbol{d} - \mathbf{K}(\hat{\boldsymbol{\theta}})\boldsymbol{a}\|_2^2 + \eta\|\boldsymbol{u}\|_1, \ \text{ s.t. } \boldsymbol{u} = \mathbf{W}_{\boldsymbol{a}}\boldsymbol{a}. \tag{7}$$

We then decompose (7) into the following subproblems, whose convergence is guaranteed by the ADMM algorithm [17]:

$$\boldsymbol{u}^{(n+1)} = \arg\min_{\boldsymbol{u}} \|\boldsymbol{u}\|_1 + \frac{\mu}{2\eta}\|\boldsymbol{u} - \mathbf{W}_{\boldsymbol{a}}\boldsymbol{a}^{(n)} - \tilde{\boldsymbol{u}}^{(n)}\|_2^2, \tag{8}$$

$$\boldsymbol{a}^{(n+1)} = \arg\min_{\boldsymbol{a}} f(\boldsymbol{a}), \tag{9}$$

$$\tilde{\boldsymbol{u}}^{(n+1)} = \tilde{\boldsymbol{u}}^{(n)} + \gamma(\mathbf{W}_{\boldsymbol{a}}\boldsymbol{a}^{(n+1)} - \boldsymbol{u}_j^{(n+1)}), \tag{10}$$

where

$$f(\boldsymbol{a}) = \|\boldsymbol{d} - \mathbf{K}(\hat{\boldsymbol{\theta}})\boldsymbol{a}\|_2^2 + \mu\|\boldsymbol{u}^{(n+1)} - (\mathbf{W}_{\boldsymbol{a}}\boldsymbol{a} + \tilde{\boldsymbol{u}}^{(n)})\|_2^2.$$

Subproblem (8) can be solved explicitly using shrinkage:

$$\boldsymbol{u}^{(n+1)} = \mathrm{shrink}(\mathbf{W}\boldsymbol{a}^{(n)} + \tilde{\boldsymbol{u}}^{(n)}, \eta/\mu),$$

where $\mathrm{shrink}(\boldsymbol{v}, \eta) = \boldsymbol{v}. * \max(1 - \eta./|\boldsymbol{v}|, 0)$, while subproblem (9) is quadratic, and can be readily solved by standard convex optimization tools.

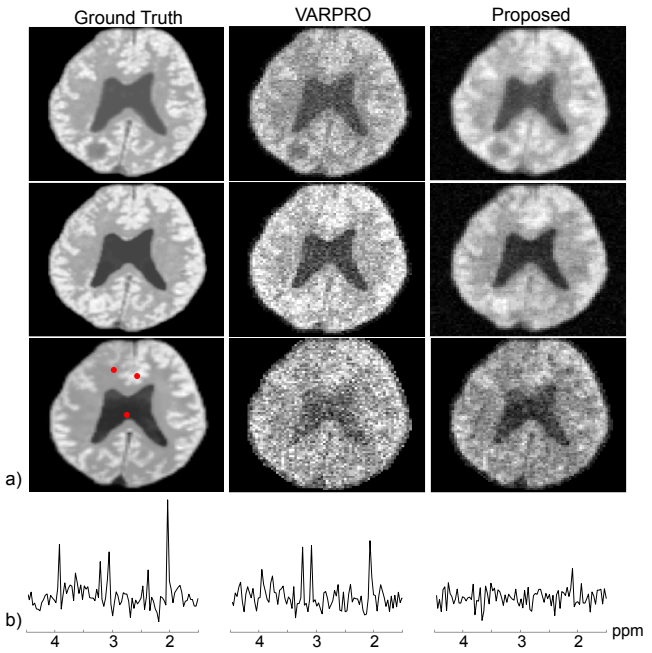

Fig. 1. Simulation results: a) the metabolite concentration maps for NAA, Creatine, and Glx (Glutamate+Glutamine), respectively; and b) three spectra at three spatial locations marked by red dots, which illustrate the SNR level of the original data. Note the improved performance (reduced spatial variation) of the proposed method over VARPRO.

3. RESULTS AND DISCUSSION

3.1. Validation with Simulated MRSI Data

We have evaluated the performance of the proposed method and compared it with VARPRO [5], a standard method used in practice. VARPRO performs spectral quantitation voxel by voxel using a set of pre-determined spectral basis, as is done in other state-of-the-art frequency-domain methods (LCModel [6], etc.) and time-domain (QUEST [7], AQSES [8], etc.) methods.

Figure 1 shows a comparison of the typical quantitation results for NAA, Creatine, and Glx (Glutamate+Glutamine) maps using VARPRO and the proposed method, respectively, on a simulation phantom dataset. The phantom was generated using the basis functions of 6 metabolites (NAA, Creatine, Choline, Glutamine, Glutamate, and myo-Inositol) obtained by quantum simulations. From Fig. 1, we can see that the estimated concentration maps by VARPRO were very noisy (large spatial variations); the proposed

method significantly reduced the estimation variance. To better illustrate the estimation results, Fig. 2 shows the synthetic spectra from the true spectral parameters and the estimated parameters for one spatial location. As can be seen, the spectrum from VARPRO parameters showed noticeable errors, which were significantly reduced by the proposed method (due to the spatial sparsity constraint).

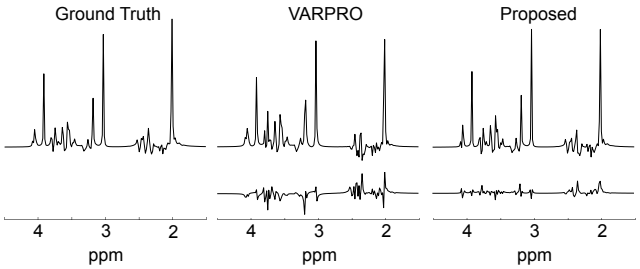

Fig. 2. Spectra generated using the true spectral parameters from the simulation phantom in Fig. 1, and the estimated parameters from VARPRO and the proposed method, respectively. The second row shows the difference between the estimated spectra and the true one. Note the reduced errors by the proposed method.

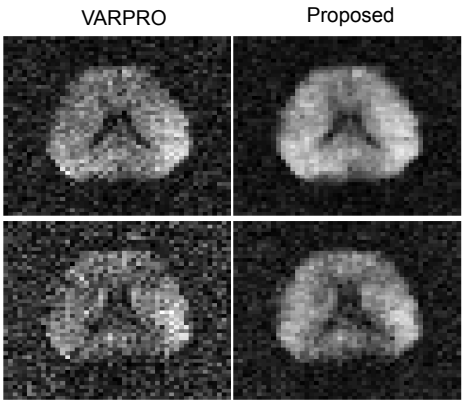

Fig. 3. Results from in vivo MRSI data. The concentration maps for two metabolites, NAA (top) and Creatine (bottom), are presented. Note that the VARPRO results show significant spatial variations (indicating large estimation variance), which are reduced considerably by the proposed method.

3.2. Validation with Experimental MRSI Data

To further validate the proposed method, an in vivo dataset was acquired from a healthy volunteer on a 3T scanner with a 30ms echo-time and 48 x 48 spatial encodings using an echo-planar spectroscopic imaging (EPSI) sequence. Figure 3 shows the NAA and Creatine maps obtained using VARPRO and the proposed method, respectively. As can be seen, the metabolite concentration maps estimated by VARPRO showed large spatial variations, including noisy "spikes" at some locations. The proposed method significantly reduced the estimation variance of VARPRO, as expected. The performance improvement of the proposed method observed from the experimental data was consistent with the simulation results in Fig. 1.

One simple idea to apply spatial regularization is to denoise the estimates of a state-of-the-art method by enforcing the spatial smoothness constraint:

$$\hat{\boldsymbol{a}} = \arg\min_{\boldsymbol{a}} \frac{1}{2}\|\boldsymbol{a} - \tilde{\boldsymbol{a}}\|_2^2 + \eta\|\mathcal{W}_{\boldsymbol{a}}\{\boldsymbol{a}\}\|_1, \tag{11}$$

where $\tilde{\boldsymbol{a}}$ denotes the current estimation of $\boldsymbol{a}$ by a state-of-the-art method. We have evaluated this method based on VARPRO, as well. As indicated by Fig. 4, such an approach can help reduce the noise, but it also introduces some blurring artifacts, and the estimates may also be biased due to non-Gaussianarity of the noise in the VARPRO results. The proposed method overcomes these problems, and perhaps more importantly, the performance of the proposed method can be much more easily characterized.

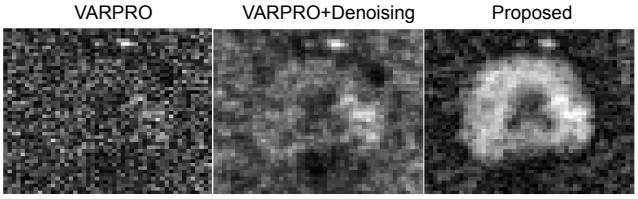

Fig. 4. Estimated concentration maps for metabolite myo-Inositol using VARPRO, denoising of VARPRO and the proposed method, respectively, from the in vivo MRSI data in Fig. 3. Note the improved performance of the proposed method over the denoising method.

3.3. Performance Analysis

For simplicity, we ignore the estimation error in $\boldsymbol{\theta}$, and treat $\boldsymbol{\theta}^*$ as the true value. It is well known that if the concentration $\boldsymbol{a}$ satisfies a certain level of transform sparsity, then a solution to (7) is also a solution to the following constrained optimization problem:

$$\hat{\boldsymbol{a}} = \arg\min_{\boldsymbol{a}} \frac{1}{2}\|\boldsymbol{d} - \mathbf{K}(\boldsymbol{\theta}^*)\boldsymbol{a}\|_2^2, \;\; \text{s.t. } \|\mathbf{W}_{\boldsymbol{a}}\boldsymbol{a}\|_0 = M. \tag{12}$$

Therefore, the performance of the proposed method can be characterized by the constrained CRB [10, 11] of (12), which is a lower bound on the variance of the estimated parameters that reside in a constrained space. Assume that $\boldsymbol{a}$ is real and $\mathbf{W}$ is invertible for convenience. The total variance for $\hat{\boldsymbol{a}}$ in (12) is bounded as [11]

$$\text{Var}(\hat{\boldsymbol{a}})_{\text{constrained}} \geq \text{Tr}(\mathbf{A}[\mathbf{A}^T\mathbf{F}_{\text{c}}\mathbf{A}]^{-1}\mathbf{A}^T), \tag{13}$$

where $\mathbf{F}_{\text{c}}$ is the Fisher information matrix, and $\mathbf{A}$ is selected to be those columns of $\mathbf{W}_{\boldsymbol{a}}^{-1}$ corresponding to the support of $\mathbf{W}_{\boldsymbol{a}}\boldsymbol{a}$. In practice, the constrained CRB is calculated using $\hat{\boldsymbol{\theta}}$ from (5). This discrepancy can be modeled as an additive perturbation, which can be characterized by a linearization of (5) and $\mathbf{K}(\boldsymbol{\theta})$.

In comparison with state-of-the-art methods, the estimator in (3) does not fix the value of nonlinear terms and has no sparsity constraint; its performance can be characterized by the unconstrained CRB:

$$\text{Var}(\hat{\boldsymbol{a}})_{\text{unconstrained}} \geq \text{Tr}(\mathbf{F}_{\text{u}}^{-1}). \tag{14}$$

To describe the theoretical improvement when using spatial constraints for quantitation, we define the ratio between the constrained CRB in (13) and the unconstrained CRB in (14):

$$R = \frac{\text{Tr}(\mathbf{F}_{\text{u}}^{-1})}{\text{Tr}(\mathbf{A}[\mathbf{A}^T\mathbf{F}_{\text{c}}\mathbf{A}]^{-1}\mathbf{A}^T)}. \tag{15}$$

We also define sparsity level as the proportion of non-zero terms of $\mathbf{W}_{\boldsymbol{a}}\boldsymbol{a}$ in (12). Figure 5 compares the improvement in CRB for spatial constraints by showing R's against different sparsity levels (red line), and the ratios between the total variance of $\hat{\boldsymbol{a}}$ from the estimator in (3) and the estimator in (7) obtained by Monte-Carlo simulations (blue line). As expected, the improvement obtained by incorporating sparsity constraint increases as the sparsity level decreases. The result of Fig. 5 is consistent with the conclusion obtained by Lam et al. [11].

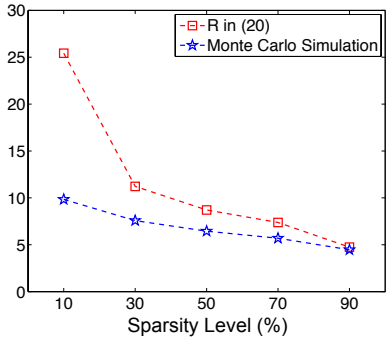

Fig. 5. Performance analysis of the proposed method imposing wavelet transform sparsity on the concentration maps. The red line is the R's in (15), while the blue line is the result of the corresponding Monte-Carlo simulations.

4. CONCLUSION

Spectral quantitation is a key problem in MRSI. Existing methods exploit only spectral prior information, and solve the problem independently for each voxel. While these methods have been successfully used in practice, their spectral estimates from MRSI data with low SNRs often have very large variances, limiting their practical utility in high-resolution MRSI studies. In this paper, we have presented a new method to address this problem. The proposed method jointly estimates the metabolite concentrations for all spatial locations, while enforcing both smoothness of the T_2^* map and transform sparsity of the metabolite concentrations. Simulation and experimental results show that the proposed method can produce significantly better spectral estimates than the state-of-the-art methods, which is consistent with the predicted performance using constrained CRB analysis. The proposed method should prove useful for spectral quantitation in various MRSI studies.

5. REFERENCES

[1] H. Barkhuijsen, R. De Beer, and D. Van Ormondt, "Improved algorithm for noniterative time-domain model fitting to exponentially damped magnetic resonance signals," *Journal of Magneic Resonance*, pp. 553–557, 1987.

[2] W. W. F. Pijnappel, A. van den Boogaart, R. de Beer, and D. van Ormondt, "SVD-based quantification of magnetic resonance signals," *Journal of Magnetic Resonance*, vol. 97, no. 1, pp. 122–134, 1992.

[3] H. Barkhuijsen, R. de Beer, W. M. M. J. Bovée, and D. van Ormondt, "Retrieval of frequencies, amplitudes, damping factors, and phases from time-domain signals using a linear least-squares procedure," *Journal of Magnetic Resonance*, vol. 61, no. 3, pp. 465–481, 1985.

[4] S. Vanhuffel, H. Chen, C. Decanniere, and P. van Hecke, "Algorithm for time-domain nmr data fitting based on total least squares," *J Magn Reson Ser A*, vol. 110, no. 2, pp. 228–237, 1994.

[5] JWC Van der Veen, R De Beer, PR Luyten, and D Van Ormondt, "Accurate quantification of in vivo ^{31}P NMR signals using the variable projection method and prior knowledge," *Magnetic Resonance in Medicine*, vol. 6, no. 1, pp. 92–98, 1988.

[6] S. W. Provencher, "Estimation of metabolite concentrations from localized in vivo proton nmr spectra," *Magnetic Resonance in Medicine*, vol. 30, no. 6, pp. 672–679, 1993.

[7] H. Ratiney, M. Sdika, Y. Coenradie, S. Cavassila, D. van Ormondt, and D. Graveron-Demilly, "Time-domain semi-parametric estimation based on a metabolite basis set," *NMR in Biomedicine*, vol. 18, pp. 1–13, 2005.

[8] J.-B. Poullet, D. M. Sima, A. W. Simonetti, B. de Neuter, L. Vanhamme, P. Lemmerling, and S. van Huffel, "An automated quantitation of short echo time mrs spectra in an open source software environment: AQSES," *NMR in Biomedicine*, vol. 20, no. 5, pp. 493–504, 2007.

[9] K. Young, V. Govindaraju, B. J. Soher, and A. A. Maudsley, "Automated spectral analysis i: Formation of a priori information by spectral simulation," *Magnetic Resonance in Medicine*, vol. 40, no. 6, pp. 812–815, 1998.

[10] Z. Ben-Haim and Y. C Eldar, "The cramér-rao bound for estimating a sparse parameter vector," *Signal Processing, IEEE Transactions on*, vol. 58, no. 6, pp. 3384–3389, 2010.

[11] F. Lam, C. Ma, and Z.-P. Liang, "Performance analysis of denoising with low-rank and sparsity constraints," in *Biomedical Imaging (ISBI), 2013 IEEE 10th International Symposium on*. IEEE, 2013, pp. 1223–1226.

[12] B. J. Soher, K. Young, A. Bernstein, Z. Aygula, and A. A. Maudsley, "GAVA: spectral simulation for in vivo mrs applications," *Journal of Magnetic Resonance*, vol. 185, no. 2, pp. 291–299, 2007.

[13] J. P. Haldar, D. Hernando, S.-K. Song, and Z.-P. Liang, "Anatomically constrained reconstruction from noisy data," *Magnetic Resonance in Medicine*, vol. 59, no. 4, pp. 810–818, 2008.

[14] K. Bredies, Karl Kunisch, and Thomas Pock, "Total generalized variation," *SIAM Journal on Imaging Sciences*, vol. 3, no. 3, pp. 492–526, 2010.

[15] Jorge Nocedal and Stephen Wright, "Numerical optimization, series in operations research and financial engineering," *Springer, New York, USA*, 2006.

[16] W. Guo, J. Qin, and W. Yin, "A new detail-preserving regularizaiton scheme," *SIAM Journal on Imaging Sciences*, vol. 7, no. 2, pp. 1309–1334, 2014.

[17] B. He, L.-Z. Liao, D. Han, and H. Yang, "A new inexact alternating directions method for monotone variational inequalities," *Mathematical Programming*, vol. 92, no. 1, pp. 103–118, 2002.